CrossMark

Hydrological Responses to Land-Use Change Scenarios under Constant and Changed Climatic Conditions

Ling Zhang[1,2] · Zhuotong Nan[3,4] · Wenjun Yu[1] · Yingchun Ge[1]

Abstract This study quantified the hydrological responses to land-use change scenarios in the upper and middle Heihe River basin (HRB), northwest China, under constant and changed climatic conditions by combining a land-use/cover change model (dynamic conversion of land use and its effects, Dyna-CLUE) and a hydrological model (soil and water assessment tool, SWAT). Five land-use change scenarios, i.e., historical trend (HT), ecological protection (EP), strict ecological protection (SEP), economic development (ED), and rapid economic development (RED) scenarios, were established. Under constant climatic condition, hydrological variations are only induced by land-use changes in different scenarios. The changes in mean streamflow at the outlets of the upper and the middle HRB are not pronounced, although the different scenarios produce different outcomes. However, more pronounced changes are observed on a subbasin level. The frequency of extreme flood is projected to decrease under the SEP scenario, while under the other scenarios, no changes can be found. Two emission scenarios (A1B and B1) of three general circulation models (HadCM3, CGCM3, and CCSM3) were employed to generate future possible climatic conditions. Under changed climatic condition, hydrological variations are induced by the combination of land-use and climatic changes. The results indicate that the impacts of land-use changes become secondary when the changed climatic conditions have been considered. The frequencies of extreme flood and drought are projected to decrease and increase, respectively, under all climate scenarios. Although some agreements can be reached, pronounced difference of hydrological responses can be observed for different climate scenarios of different GCMs.

Keywords Hydrological response · Land-use change · Climate change · Heihe River basin · Dyna-CLUE · SWAT

Introduction

Since the 1990s, many international organizations, including the World Climate Research Programme (WCRP), International Hydrological Programme (IHP), Global Water System Project (GWSP), and International Geosphere and Biosphere Programme (IGBP), have implemented a series of water-related projects. Their objectives are to investigate the impacts of environmental changes on hydrologic cycles and related resources at the global, regional, and catchment scales (Xia and Tan 2002; Li et al. 2013). The investigation of the hydrologic responses to environmental changes has become a hotspot topic, especially within the water science community (Xia and Tan 2002).

Land-use changes, which represent a type of active environmental factor, have significant impacts on hydrological processes, such as evapotranspiration (ET), soil infiltration, and precipitation interception (Hurkmans et al. 2009; Im et al.

✉ Zhuotong Nan
nanzt@njnu.edu.cn

1 Cold and Arid Regions Environmental and Engineering Research Institute, Chinese Academy of Sciences, Lanzhou 730000, People's Republic of China

2 University of Chinese Academy of Sciences, Beijing 100049, People's Republic of China

3 School of Geography Science, Nanjing Normal University, Nanjing 210023, People's Republic of China

4 Jiangsu Center for Collaborative Innovation in Geographical Information Resource Development and Application, Nanjing 210023, People's Republic of China

2009). Unlike physical catchment characteristics, such as topography and soil properties, the land-use changes are more likely to result in short-term hydrologic variations (Elfert and Bormann 2010). Thus, numerous recent studies have investigated hydrological responses to land-use changes. Wijesekara et al. (2012) explored the hydrological responses to future Land Use and Land Cover Changes (LUCCs) in the Elbow River watershed of Canada, while Baker and Miller (2013) examined the hydrological responses to historical LUCCs in the River Njoro watershed of Kenya. Nie et al. (2011) and Zhou et al. (2013) found that surface runoff is very sensitive to urbanization and that land-use changes have significant effects on hydrological processes. The results of those studies can be used to improve the predictability of hydrological responses to land-use changes, which can be useful for decision making. However, many of these studies have assumed that the local climate remained constant in the simulation period. In fact, climate change is another active factor that can even have larger effects on hydrological processes than those induced by land-use change (Kim et al. 2013; Khoi and Suetsugi 2014). Recently, many studies have assessed the impacts of climate change on hydrological variations, e.g., Ficklin et al. (2013), Perazzoli et al. (2013), Xu et al. (2013b), and Ashraf Vaghefi et al. (2014). These studies found that climate change can impact the hydrologic cycle substantially. For example, Ashraf Vaghefi et al. (2014) studied the effects of climate change on water source in the Karkheh River basin of Iran, in which the freshwater availability was projected to change significantly due to climate change. Xu et al. (2013b) reported that a decreased trend of runoff would be found in the upper reaches of the Qiantang River basin as a result of climate change. Similar results were found in the Mono Lake (Ficklin et al. 2013) and Concórdia River basins (Perazzoli et al. 2013). The effects of land use and climate change are theoretically interlinked and cannot be completely separated (Mango et al. 2011; Tong et al. 2012). Land-use change in conjunction with climate change will undoubtedly complicate the hydrological responses solely caused by land-use change. Therefore, it is necessary to investigate the hydrological responses to land-use changes under changed climatic conditions.

Hydrological models, especially physically based spatially distributed hydrological models, have been frequently applied to quantify the hydrological responses to land-use changes. Among them, the Soil and Water Assessment Tool (SWAT) is notable because of user-friendly interface, minimum input data, and its capacity to provide continuous, long-term simulations. The SWAT model has been widely used in different catchments across the world and at different scales (e.g., Nejadhashemi et al. (2011), Du et al. (2013), Shi et al. (2013), and Wang et al. (2014). Those studies proved that the SWAT model can be used as an effective tool to examine hydrological responses to land-use changes.

Recently, a handful of studies have emphasized the advantages of an integrated approach in accurately evaluating the effects of land-use changes on hydrological processes. Chu et al. (2010) investigated the effects of dynamic land-use changes on streamflow, groundwater, and soil moisture in the Rhine basin by combining the distributed hydrology-soil vegetation (DHSVM) model and the conversion of land use and its effects (CLUE-s) model. Wijesekara et al. (2012) coupled the physically based MIKE SHE/MIKE-11 hydrological model with the land-use cellular automata (CA) model to investigate the effects of land-use changes on hydrological processes in the Elbow River watershed. Zhou et al. (2013) examined hydrological responses to urbanization in the Yangtze River Delta region by coupling the CLUE-s model with the SWAT model. Such combination of land-use change model and hydrological model not only facilitates the investigation of land-use change impact on hydrological processes, but also enables the exploration of various hydrological variation trajectories; the latter could benefit authorities and stakeholders in making science based policies and decisions.

As the second largest inland river basin in the arid region of northwestern China, the Heihe River basin (HRB) sustains millions of people. Recently, drastic LUCCs have occurred in the upper and middle HRB (Fig. 1), especially in the middle HRB, which is the most developed area in HRB. These changes have been driven by increasing population, urbanization, economic development, and industrialization. As a result, this area has faced severe long-term problems related to water resources, such as water shortages and irrational utilization, which constrain the sustainable development of local economy and society, and hinder the effective implementation of ecological protection (Li et al. 2009; Nian et al. 2014). Understanding and modeling hydrological responses to various land-use change scenarios are very important for optimizing the planning, policy-making, and management of land use and water resources. However, very limited studies have been conducted to explore the effects of land-use changes on hydrological responses in the HRB. Wang et al. (2005) and Zhou et al. (2013) studied the middle HRB, analyzing the effects of land-use changes on the groundwater. Wang et al. (2007) investigated the effects of land-use changes on runoff processes in HRB. However, neither of these studies investigated the effects of land-use changes on a model basis or the effects of various land-use change scenarios. The existing studies which have explored the hydrological responses to climate change in HRB are based on long-term historical data using statistical methods (Zhang et al. 2007; Wang and Zhang 2010). No hydrological model such as SWAT was employed to assess climatic impacts. Moreover, few studies have investigated the combined impacts of land use and climate change on hydrologic circle.
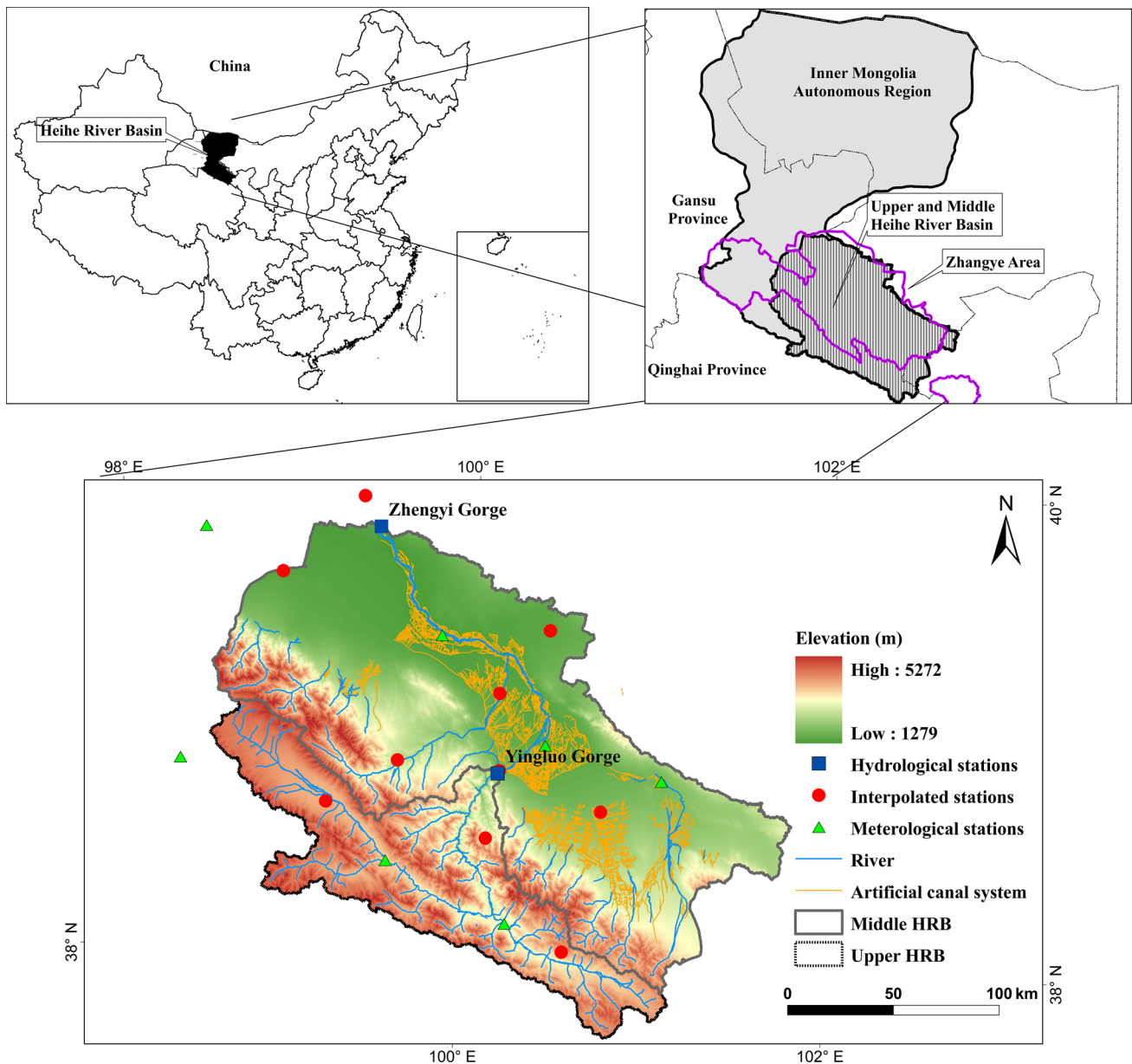
Fig. 1 Location of the study area and the distribution of hydro-meteorological stations (Color figure online)

Taking the upper and middle HRB as the study area, the overall objective of this study is to investigate the hydrological responses to land-use change scenarios under both constant and changed climatic conditions. Specifically, we seek to (1) simulate land-use patterns from 2010 to 2039 under five different scenarios, i.e., historical trend (HT), ecological protection (EP), strict ecological protection (SET), economic development (ED) and rapid economic development (RED) scenarios; (2) identify hydrological contributions of each single land-use class; and (3) quantify hydrological responses to different land-use change scenarios under constant climatic conditions; and (4) examine hydrological responses to land-use changes under changed climatic conditions, represented by two climate scenarios

(A1B and B1) of three general circulation models (HadCM3, CGCM3, and CCSM3). The results of this study will provide quantitative information for authorities and stakeholders in planning and managing land and water resources in HRB and also can be used as a reference for similar inland river basins in arid regions worldwide suffered common water stress problems.

Study Area

The Heihe River basin (HRB), bounded by longitudes 98° and 101°30′E and latitudes 38° and 42°N, covers an area of approximately 128,000 sq. km. The river flows from south

to north across three provinces in China, i.e., Qinghai, Gansu and Inner Mongolia. The basin comprises three parts, namely the upper, middle and lower HRB, with gages at Yingluo Gorge and Zhengyi Gorge stations. The upper and middle HRB, extending from Qilian Mountains, the source of the Heihe River, to the Zhengyi Gorge, the outlet of the middle reach, are selected as the study area (Fig. 1).

As a primary contributing area of runoff, the upper HRB with an outlet at the Yingluo Gorge, covers an area of approximately 9760 sq. km, and has typical mountainously geographic, climatic and ecological features. The elevations range 2000–5500 m; the main vegetation types include alpine forest and grassland; the mean annual precipitation is 250–500 mm (Li et al. 2001); and the mean annual evaporation is approximately 700 mm (Wang and Zhang 2010). The middle HRB refers to the area of approximately 25,684 sq. km between the Yingluo Gorge and Zhengyi Gorge. As a primary area of water consumption, this region has been well developed, with millions of people living in oases (Zhang et al. 2015). The elevations range 1000–2000 m; the main vegetation type is artificially planted vegetation; the mean annual precipitation decreases from 250 to 50 mm from south to north (Zang and Liu 2013); and the annual potential evaporation changes northward from 2000 to 4000 mm (Wang and Zhang 2010). With a large area of irrigated land, the oases in the middle HRB are becoming a highly developed agricultural district with a long agriculture history dating back nearly 2000 years (Wang et al. 2014). This area is well known as an important grain-producing region in northwestern China. To effectively utilize and manage available, yet limited, water resources, an intensive and advanced artificial canal system for irrigation has been constructed. Six primary land-use types, i.e., cultivated land, forest, grassland, water body, developed land, and unused land, exist in the study area. They were mapped on basis of visual interpretation and expertise from Landsat MSS, TM, and ETM + satellite images (Wang et al. 2011). Grassland and unused land occupy 72.44 % of the total land area (Table 1), followed by forest, which accounts for 13.18 %. Cultivated land, water body, and developed land constitute the remaining 14.38 %.

Materials and Methods

Overview

The implementation of the selected land-use change model, dynamic conversion of land use and its effects (Dyna-CLUE), is presented, followed by a detailed description of the scenarios settings. The physically based spatial distributed hydrological model, SWAT, is then described with respect to its configuration, inputs, and the methodology of calibration and validation. The method to project future climatic conditions in the study area is then presented. This section ends with the hydrological assessment of each single land-use class and the coupling of LUCC and hydrological models in order to quantify hydrological responses to land-use changes under both constant and changed climatic conditions.

Modeling Land-Use Changes under Different Scenarios

LUCC Model

The LUCC model, Dynamic Conversion of Land Use and its Effects (Verburg et al. 2002; Verburg and Overmars 2009), was selected to simulate dynamic land-use changes under different scenarios. Specifically, trend extrapolation was used to calculate the demands of each land-use type for each year during the simulation period (Verburg et al. 2006). Then, the Dyna-CLUE model was used to transform the demands into each location of the study area according to the conversion rules and the total probability of each land-use type.

The conversion rules include spatial restrictions and a conversion matrix. The spatial restrictions define areas that are not permitted to be converted, whereas the conversion matrix describes the convertibility between land-use types. In this study, we defined forest and grassland areas with slopes exceeding 25 % as restricted areas in compliance with the China's laws. In addition, we restricted the convertibility from developed land to any other land-use types and from any other type to water body.

The total probability of each land-use type is a sum of the spatial suitability, neighborhood suitability, conversion elasticity, and competitiveness. In this study, the spatial suitability for a specific land-use type was estimated using a stepwise logistic regression (Eq. 1) based on the relationship between the land-use pattern in 1986 and a set of driving factors (Serneels and Lambin 2001; Gobin et al. 2002).

$$\text{Log}\left(\frac{P_i}{1 - P_i}\right) = \beta_0 + \beta_1 X_{1,i} + \beta_2 X_{2,i} + \cdots + \beta_n X_{n,i} \quad (1)$$

where P_i is the location suitability of a grid cell (i) for the occurrence of the considered land-use type, X is the driving factors, and β is the regression coefficient of each driving factor. The selected driving factors include elevation, slope, aspect, soil type, distance to the nearest road, distance to the nearest railway, distance to the nearest river, distance to the nearest reservoir, distance to the nearest residential area, GDP per land area, GDP per capita, and population density.

Table 1 Summary of land use in the study area in 2000

Land use type	Description	Area (ha)	Percentage
Cultivated land	Dry land and paddies	394,200	11.12
Forest	Timber, shelter, and economic forest; sparse woodland and shrub	467,001	13.18
Grassland	High (>50 %), medium (20–50 %) and low (5–20 %) grassland coverage	1,281,195	36.15
Water body	River, lake, reservoir, permanent glacier, and snow	81,504	2.30
Developed land	Land for residence, enterprise, mining, and transportation	33,984	0.96
Unused land	Sandy land, desert, saline land, bare land, the Gobi, and other lands	1,286,406	36.29

Similar to the spatial suitability, the neighborhood suitability for a specific land-use type was also estimated via a stepwise logistic regression based on the land-use data and the selected enrichment factors (Verburg et al. 2004). The conversion elasticity is typically used to describe the stability of a land-use type, i.e., it measures the level of difficulty for converting one land-use type to another. The conversion elasticity values were set to 0.8, 0.6, 0.6, 0.9, 1, and 0.4 for cultivated land, forest, grassland, water, developed land, and unused land, respectively, by referring to the relevant literatures (Verburg et al. 2002; Xu et al. 2013a) and the actual land-use changes observed from 1986 to 2000 in the study area. The competitiveness is an iteration variable that represents the competitive advantage. In an iterative procedure, it would be assigned a lower value if the allocated area is greater than area demanded, and vice versa.

Before applying the Dyna-CLUE model to the study area, the actual land-use maps for the entire HRB in 2000 and the Zhangye administrative area (Fig. 1), located in the middle HRB, in 2000 and 2005 were used for model validation. As the Zhangye area's boundaries do not exactly match the study area, only overlapped areas are compared. The overall accuracy, Kappa coefficient and producer's accuracy were adopted for evaluation. Higher overall accuracy and Kappa coefficient indicate higher similarity between the actual map and the simulated map. Likewise, larger producer's accuracy indicates greater similarity between the pair of classes tested. All of the land-use data and driving factors discussed above were collected from the Scientific Data Center in Cold and Arid Regions (http://westdc.westgis.ac.cn/).

Scenario Settings

In this study, five different scenarios that represent a range of tradeoffs between ecological protection and economic development, were developed by referring to the relevant literature and government planning (The Ministry of Water Resources of the People's Public of China 2000; Fang and Bao 2004; Shanghai Urban Planning & Design Institute and Zhangye Urban Construction Commission 2004; The People's Government of Zhangye 2012; Dai and Zhang 2013). The regional planning, namely Recent Management Planning of HRB (The Ministry of Water Resources of the People's Public of China 2000), Urban Planning Outline of Zhangye City for 2004 to 2020 (Shanghai Urban Planning & Design Institute and Zhangye Urban Construction Commission 2004) and Development Planning Outline of Zhangye City toward a Well-being and Tourist City for 2012 to 2020 (The People's Government of Zhangye 2012), provide reference bases for scenario setting. The major characteristics of land-use demands in each scenario are listed as follows:

(1) *Historical Trend (HT) Scenario* Future land-use demands are assumed to follow the actual linear trend from 1986 to 2000. The demands for cultivated land, developed land, and unused land will increase, and those for forest and grassland will decrease. This scenario represents the conditions without interventional policy being made for land-use changes in the near future.

(2) *Ecological Protection (EP) Scenario* The annual growth rate of the demands for cultivated land, developed land, forest, and grassland areas are assumed to be half of those under the HT scenario. To some extent, this scenario is in line with the supportive development patterns presently put forth by the national and local government programs.

(3) *Strict Ecological Protection (SEP) Scenario* The annual growth rate of the demands for cultivated land, forest, and grassland areas are set to 0.12, 1.46 and 0.27 %, respectively, following the simulation results of the coupled water–ecology–economy-coordinated development model in the HRB by Fang and Bao (2004). The demand for developed land is assumed to be similar to that of the EP scenario. This scenario is an extreme scenario that is very beneficial for the ecological environment.

(4) *Economic Development (ED) Scenario* The demands for grassland and forest areas are assumed to be

weak, whereas those for both cultivated and developed lands are assumed to be strong. Specifically, the growth rates are assumed to be double those which are under the HT scenario. To some extent, this scenario reflects a current development pattern in local area, which pursued maximum economic profits and ignored ecological protection.

(5) *Rapid Economic Development (RED) Scenario* The demand for developed land is assumed to be drastic. Specifically, developed land is assumed to grow at an annual rate of 7 %, which is in accordance with the study conducted by Dai and Zhang (2013). Meanwhile, the demands for cultivated land, grassland, and forest areas are assumed to be the same as those under the ED scenario. This scenario is an extreme scenario that is very beneficial for economic development.

The demand for water body areas is assumed to be constant after 2000, while that for unused land is assumed to be equal to the remaining area under all scenarios. The land-use patterns under different scenarios from 2000 to 2039 were then simulated using the Dyna-CLUE model.

Hydrological Model

The soil and water assessment tool has been developed to predict the effects of land management practices on water, sediment, and agricultural chemical yields in large complex watersheds with varying soils, land use and management conditions over long periods of time (Neitsch et al. 2011). As a deterministic model, each run of SWAT will produce exactly same outputs with same inputs. This feature makes the model preferred for isolating the contributions of a variable, such as climate change or land-use change, to hydrological responses (Baker and Miller 2013).

A digital elevation model (DEM), land-use and land-cover information, soil type map and soil properties, and observed meteorological data are required by the SWAT model to simulate the hydrological processes. All input data used in this study, except the observed meteorological data, were provided by the Scientific Data Center in Cold and Arid Regions. The meteorological data (1970-2009), including daily precipitation, maximum temperature, minimum temperature, wind speed, relative humidity, and solar radiation at nine weather stations (i.e., Dingxin, Jiuquan, Gaotai, Zhangye, Shandan, Tuole, Yeniugou, Qilian, and Yongchang), were provided by the China Meteorological Data Sharing Service System (http://data.cma.cn/).

Only a few precipitation stations are available in this large study area, and it is unable to accurately capture the real distribution of precipitation, especially in the mountainous upper HRB. Thus, we chose ten locations (see Fig. 1) with varying elevations and interpolated their precipitation time series using the tool known as meteorological distribution system for high-resolution terrestrial modeling (MicroMet), in the hope of improving the simulation accuracy of SWAT (Liston and Elder 2006). To consider the effects of the artificial canal system across the middle HRB, several implementations were made in the SWAT model by referencing to the work of Lai et al. (2013). First, due to the fact of the canal system being the main source of water consumption in the middle HRB, the irrigation parameters in the model were adjusted to match the actual use of canal system from statistic books recorded by local water bureau. Second, being aware of the existence of frequent interaction between surface water and ground water due to irrigation, which will consequently lead to lower streamflow simulation at the outlet of the middle HRB during the period that irrigation is stopped and ground water recharges the river, such as winter, the infiltration equations were therefore modified to increase the ground water recharge in order to balance water.

The irrigation will heavily impact the water balance in the soil layer. The soil moisture content is calculated using Eq. 2.

$$\text{SOL\_SW}_t = \sum_{i=1}^{n} \text{SOL\_SW}(i) \times (1 - \alpha) \qquad (2)$$

where SOL_SW_t is the moisture content contained in the entire soil profile, t is the current timeslot, $\text{SOL\_SW}(i)$ is the moisture content of the layer i and α is the empirical coefficient of infiltration which was set as a constant at 0.007 in our case.

The percolation of the bottom soil layer is then calculated using Eq. 3.

$$W_{\text{perc,bm}} = \text{SW\_EX}_{\text{bm}} \times \left[1 - \exp\left(\frac{-\Delta t \times K_{\text{sat,bm}}}{\text{SAT}_{\text{bm}} - \text{FC}_{\text{bm}}}\right) \right]$$
$$+ \alpha \times \sum_{i=1}^{n} \text{SOL\_SW}(i) \qquad (3)$$

where $W_{\text{perc,bm}}$ is the percolation amount of the bottom soil layer, Δt is the time step, $K_{\text{sat,bm}}$ is the saturated hydraulic conductivity of the bottom layer, SAT_{bm} is the saturated field capacity of the bottom layer, FC_{bm} is the field capacity of the bottom soil layer, and SW_EX_{bm} is the soil moisture exceeding its field capacity.

In this study, the SWAT model was calibrated using a "trial and error" procedure (Im et al. 2009) based on the land-use map of the year of 2000 and the observed monthly streamflow at two gage stations: Yingluo Gorge (1990–1999) and Zhengyi Gorge (2000–2004). The multigage calibration can enhance the calibration results from the perspective of spatial variations in the hydrological responses (Park et al. 2011). After model calibration,

additional 10 years (2000–2009) of records from Yingluo Gorge station and 5 years of records from Zhengyi Gorge station were used for model validation. The results were assessed by two indices, namely the Nash–Sutcliffe efficiency (NSE) (Nash and Sutcliffe 1970) and the coefficient of determination (R^2). NSE ranges between negative infinity and 1 (inclusive) and R^2 ranges from 0 to 1. Higher NSE and R^2 mean better model performance. The NSE and R^2 are expressed in Eqs. 4 and 5.

$$\text{NSE} = 1 - \frac{\sum_{i=1}^{n}(Q_i^{\text{obs}} - Q_i^{\text{simu}})^2}{\sum_{i=1}^{n}(Q_i^{\text{obs}} - Q_{\text{obs}}^{\text{mean}})^2} \tag{4}$$

$$R^2 = \left(\frac{\sum_{i=1}^{n}(Q_i^{obs} - Q_{obs}^{mean})(Q_i^{simu} - Q_{sim}^{mean})}{\sqrt{\sum_{i=1}^{n}(Q_i^{obs} - Q_{obs}^{mean})^2}\sqrt{\sum_{i=1}^{n}(Q_i^{simu} - Q_{sim}^{mean})^2}} \right)^2 \tag{5}$$

where n is the number of time steps; Q_i^{obs} and Q_i^{sim} are, respectively, the observed and simulated streamflows at time step i; and $Q_{\text{obs}}^{\text{mean}}$ and $Q_{\text{sim}}^{\text{mean}}$ are, respectively, the mean observed and simulated streamflows over the evaluation period.

Future Climatic Conditions

Climatic projections of three general circulation models (GCMs) for two emission scenarios of the Special Report on Emission Scenarios (SERS) published by the Intergovernmental Panel on Climate Change (IPCC), as listed in Table 2, were used to represent the future climate conditions of the study area. The A1B scenario (medium emission), which emphasizes economic development, describes a future world of rapid economic growth and technological innovation, global population that peaks in the midcentury and declines thereafter, convergent development among regions, and balanced energy policies. The B1 scenario (low emission), which emphasizes environmental protection, describes a balanced world with the same population growth as in the A1B scenario, but with rapid changes in economic structures toward a service and information economy, with reductions in material intensity, the introduction of clean and resource-efficient technology, and emphasis on social justice and environmental protection.

It is well known that the resolution of GCMs is quite coarse, often between 250 and 600 km. Thus, it is essential to downscale the GCM output to force the hydrological model at a regional or watershed scale. Three downscaling methods, namely dynamic downscaling, statistical downscaling, and the Delta method, are often used (Guo et al. 2012). The Delta method was used to construct the climatic conditions from 2010 to 2039 in the upper and middle HRB under the A1B and B1 scenarios in this study. The principle of the Delta method is to apply the relative or absolute changes in meteorological elements in each grid box projected by the chosen GCM between two periods to estimate future climatic conditions at a regional or watershed scale (Wilby et al. 1999; Hay et al. 2000; Diaz-Nieto and Wilby 2005). We downscaled two meteorological variables, namely temperature and precipitation, as the changes of them are the primary controlling factors for the watershed-scale hydrological processes (Tanzeeba and Gan 2012). The data of mean monthly precipitation and temperature for the 20th century simulation (20CM3) from 1970 to 1999 and for the emission scenario (A1B and B1) from 2010 to 2039 were collected from Data Distribution Centre of IPCC (http://www.ipcc-data.org/). The change fields of mean monthly precipitation (relative change) and mean monthly temperature (absolute change) centered on two 30-year periods (1970–1999, 2010–2039) of different GCMs were then calculated. These GCM changes were employed to adjust the observed data (1970–1999) of the meteorological stations within and around the upper and middle HRB to get the 2010-2039 climate scenarios for each GCM.

Hydrological Responses to Land-use and Climate Changes

Hydrological Contributions of Single Land-Use Class

To understand the hydrological responses to land-use change scenarios, it is essential to identify the hydrological contributions of each single land-use class. Assumed that

Table 2 GCMs and SERES scenarios for future climatic projection

Center	Model	Emission scenarios	Spatial Resolution	
			Longitude	Latitude
UK Meteorological Office, UK	HadCM3	A1B, B1	3.750°	2.500°
Canadian Center for Climate Modeling and Analysis, Canada	CGCM3 (T47)	A1B, B1	3.750°	3.711°
National Centre for Atmospheric Research, USA	CCSM3	A1B, B1	1.406°	1.401°

only a single land-use class was present in the upper HRB, the hydrological responses to that land-use class were simulated from 1980 to 2009 using the validated SWAT model. The model configuration is identical for each run to ensure the differences between hydrological responses are only induced by the differences of land use. The class of water body was excluded from this testing. The simulated average hydrological components, including surface run-off, lateral flow, groundwater, ET, and water yield, were compared to examine the hydrological contributions of each single land-use class.

Scenario-Based Simulation

Hydrological responses to land-use changes under both constant and changed climatic conditions were investigated. A baseline scenario was introduced to serve as a reference scenario that assumes the climate regime will be kept at the historical level (i.e., 1980–2009) and land use will preserve the pattern observed in 2000. Under constant climatic condition, the climatic condition was assumed to be same with the baseline scenario. The Dyna-CLUE and SWAT models were one-way coupled, i.e., the projected land-use patterns in 2015, 2025, and 2035 for different scenarios were incorporated into the SWAT model while keeping the other model configurations the same. The results were then compared herein with the baseline scenario. As a result, hydrological variations, i.e., changes in streamflow and hydrological extremes, were solely induced by the land-use changes under different scenarios. Under changed climatic condition, on the other hand, the climatic condition was assumed to be changed following the GCM projections. The meteorological data (2010–2039) of two emission scenarios (A1B and B1) projected by three GCMs, namely HadCM3, CGCM3, and CCSM3, were used to drive the SWAT model while fixing other configurations as those under constant climatic condition. In this setting, hydrological variations relative to baseline scenario are caused by both land-use and climate changes.

The hydrological extremes, i.e., extreme flood and drought, were assessed by means of frequency analysis (Lehner et al. 2006; Fotakis et al. 2014). The annual peak and minimum streamflow at the Yingluo Gorge station were retrieved from modeled daily outputs in the baseline (1980–2009) or future (2010–2039) periods. Then, the Pearson Type III (PT III) distribution, a widely applied distribution function in both flood and drought assessments, was fitted using the selected 30-year peak or minimum streamflow. The PT III peak-flow distribution was employed for extreme flood assessment, while the PT III minimum-flow distribution was used for extreme drought assessment. The changes in extreme hydrological events can be assessed by comparing the distributions of PT III peak-flow or minimum-flow simulated with different land-use scenarios and climatic conditions.

Results

Land-Use Changes under Different Scenarios

The validation results of the Dyna-CLUE model in the upper and middle HRB and the Zhangye area in the middle HRB are shown in Table 3. Overall accuracy and Kappa coefficient are 0.92 and 0.89, respectively, for the whole study area in 2000. Both of these metrics exceed 0.85, indicating a good agreement between the actual and simulated land-use maps. This agreement is once more confirmed when we compared the actual and simulated land-use maps for the Zhangye area in 2000 and 2005. Overall accuracy and Kappa coefficient are 0.92 and 0.89, respectively, in 2000; and 0.90 and 0.86, respectively, in 2005. All land-use types except for developed land have high producer's accuracy for the three maps within the study area. The relative low accuracy of developed land is mainly because its changes are subject to the effects of many social–economic factors, which were not fully taken into account in the model. The validation results indicate that the Dyna-CLUE model performs well in the study area and can be reliably used for projecting land-use changes.

Land-use changes under different scenarios, namely the HT, EP, SEP, ED, RED scenarios, in comparison with the visually interpreted land-use map of 2000, are shown in Fig. 2. The simulated land-use patterns under the two extreme scenarios, i.e., SEP and RED, exhibit pronounced differences compared to the other simulated maps. For the

Table 3 Validation results for the Dyna-CLUE model

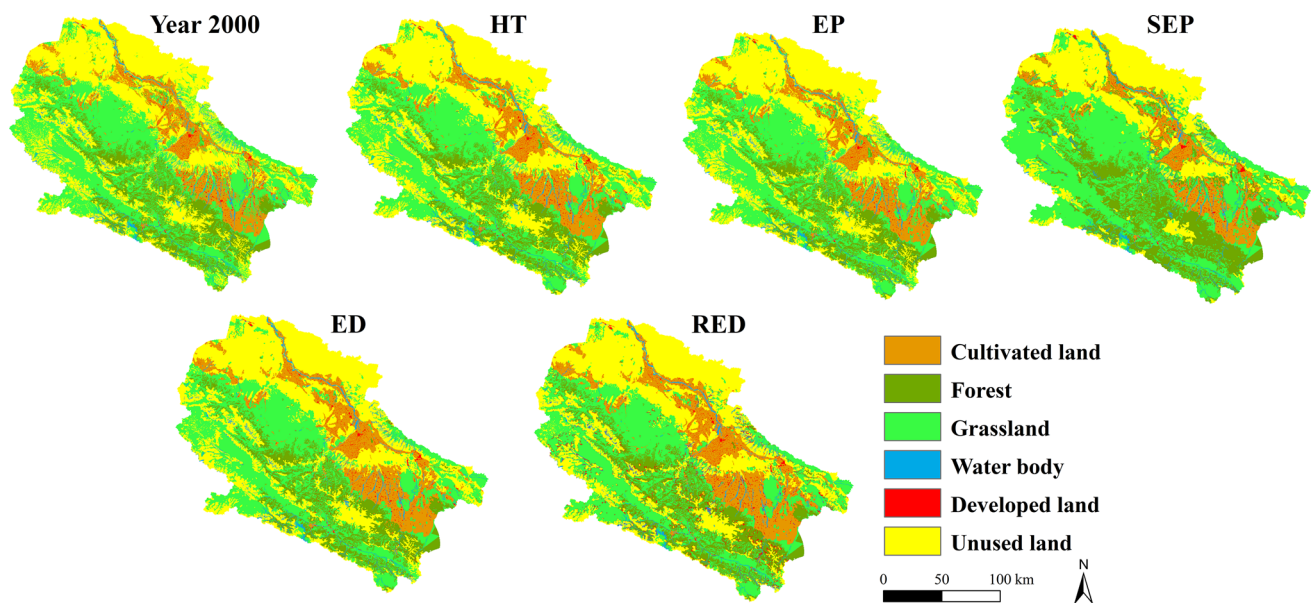| Region and year	Overall accuracy	Kappa Coefficient	Producer's accuracy					
			Cultivated land	Forest	Grassland	Water body	Developed land	Unused land
The upper and middle HRB in 2000	0.92	0.89	0.89	0.90	0.92	0.83	0.75	0.94
Zhangye area in the middle HRB in 2000	0.92	0.89	0.89	0.90	0.91	0.82	0.75	0.95
Zhangye area in the middle HRB in 2005	0.90	0.86	0.83	0.88	0.89	0.72	0.71	0.95

Fig. 2 Actual land-use map in 2000 and the simulated maps in 2039 for different scenarios (Color figure online)

Table 4 Relative (%) and absolute (hectare) changes of each land-use type in the upper and middle HRB under different scenarios from 2000 to 2039

Land-use type	HT	EP	SEP	ED	RED
Cultivated land	15.50 % (61,083)	7.76 % (30,591)	−4.61 % (18,189)	30.90 % (121,806)	30.64 % (120,789)
Forest	−3.79 % (−17,703)	−1.77 % (−8262)	57.00 % (266,193)	−7.54 % (−35,217)	−7.07 % (−33,039)
Grassland	−4.35 % (−55,674)	−2.17 % (−27,792)	10.55 % (135,153)	−8.72 % (−111,708)	−8.69 % (−111,285)
Water body	−0.42 % (−342)	−0.32 % (−261)	−0.08 % (−63)	−0.56 % (−459)	−1.87 % (−1521)
Developed land	8.18 % (2781)	2.57 % (873)	2.22 % (756)	18.22 % (6192)	262.13 % (89,082)
Unused land	0.77 % (9855)	0.38 % (4851)	−29.84 % (−383,850)	1.51 % (19,386)	−4.98 % (−64,026)

SEP scenario, the distribution of forest and grassland in 2039 is much broader than in the other scenarios. However, for the RED scenario, more developed land appears, especially in the upper HRB, compared with the other scenarios. The simulated land-use patterns in 2039 under the HT, EP and ED scenarios only show slight difference from the pattern in 2000.

The absolute and relative changes in each land-use type in the upper and middle HRB between 2000 and 2039 under different scenarios are listed in Table 4. Under the HT scenario which represents the current condition, cultivated land exhibits a pronounced increasing trend, whereas both grassland and forest exhibit a decreasing trend. The changes of water body and developed land are not substantial. The results indicate that the increase in cultivated land area comes primarily at the expense of grassland and forest areas, which would lead to the degeneration of the ecological environment. Furthermore, unused land, which primarily includes sandy land, desert, saline land, bare land, the Gobi, and other lands, presents an increasing

trend, indicating that the ecological environment would further deteriorate if no control is enforced. Land-use changes under HT highlight the fact that if no measures are taken to control the growth of cultivated land area, which otherwise is at the cost of compromising the economic development, the fragile HRB ecosystem will face a serious threat. Under the EP scenario (Table 4), the increase in cultivated land area and the decrease in forest and grassland areas are controlled to some extent by limiting their demands under this scenario. Although this result expresses an encouraging sign, it is not so much optimistic and near-future land-use changes remain uncertain if local government does not fully implement the policies. Under the SEP scenario, which is designed as an extreme scenario very beneficial to the ecological environment, the areas of grassland and forest show a substantial increase trend, whereas unused land area exhibits a pronounced decrease trend. The results suggest that theoretically an effective way to protect ecological lands is to recover unused land by replanting trees and grasses if with sufficient water supply.

For the ED scenario, which represents to some degree an ongoing economic development pattern in the study area, the expansion of cultivated land and the decrease in grassland and forest areas are more substantial than in the HT and EP scenarios. The results highlight the fact that if the current development pattern is continuing, future ecological environment will be pessimistic. The RED scenario, in contrast to the SEP scenario, is also an extreme scenario very beneficial for economic development, under which developed land area increases without control. Although this scenario is unlikely to happen, it cautions us about the necessity of managing land resources.

Calibration and Validation of SWAT

Table 5 shows the calibration and validation results of the monthly streamflow at the Yingluo Gorge and Zhengyi Gorge stations. NSE and R^2 at the Yingluo Gorge station are 0.90 and 0.92, respectively, for the calibration period, and 0.88 and 0.89 for the validation period. Figure 3 compares the simulated and observed monthly streamflows at the Yingluo Gorge station, the outlet of the upper HRB. The results indicate that the SWAT model can simulate the streamflow very well. However, the agreement between the observed and simulated streamflows from March to May in most years is relatively poor. One explanation is that snowmelt and permafrost during these months have large effects on the streamflow; those processes that are not well

represented in the SWAT model. Furthermore, model assumptions such as no water entering deep aquifer and some techniques such as the Thiessen Polygon, used for meteorological data interpolation, jointly contribute to the simulation uncertainty. Figure 4 shows the performance of the SWAT model at the Zhengyi Gorge station, where NSE and R^2 are 0.67 and 0.75, respectively, for the calibration period, and 0.59 and 0.72 for the validation period. The simulation accuracy is lower than Yingluo Gorge. This result is caused by the complex irrigation canal system in the middle HRB, which heavily impacts on runoff generation. Although we accordingly enhanced the model and adjusted the irrigation parameters, the adverse effects cannot be eliminated completely. Nevertheless, according to the criteria proposed by Moriasi et al. (2007), the SWAT model can be applied to examine the hydrological responses to land-use changes in view of satisfactory simulations it makes.

Hydrological Contributions of Single Land-Use Class

The averaged simulated hydrological components for each land-use type hypothetically uniform in the upper HRB from 1980 to 2009 are shown in Fig. 5. Developed land has the strongest runoff yield capacity because of its extensive impervious area with low interception and infiltration capacity (Dixon and Earls 2012). Unused land is strong in runoff and water yield capacities due to low ET and interception caused by its low vegetation coverage (Fohrer et al. 2001; Wan and Yang 2005). On contrast, forest areas exhibit strong interception, infiltration, and ET capacities (Sriwongsitanon and Taesombat 2011). Furthermore, forest litter increases the surface roughness, which enhances water retention (Wen et al. 2013). Thus, the runoff and water yield capacities in forest areas are the lowest among those land-use types. Cultivated land and grassland areas have high ET capacity as well. Consequently, they present

Table 5 Calibration and validation statistics at two hydrological stations in the upper and middle HRB

Station	Simulation period	NSE	R^2
Yingluo Gorge	Calibration for 1990–1999	0.90	0.92
	Validation for 2000–2009	0.88	0.89
Zhengyi Gorge	Calibration for 2000–2004	0.67	0.75
	Validation for 2005–2009	0.59	0.72

Fig. 3 Observed and simulated monthly streamflows during the calibration and validation periods at the Yingluo Gorge station (outlet of the upper HRB) (Color figure online)
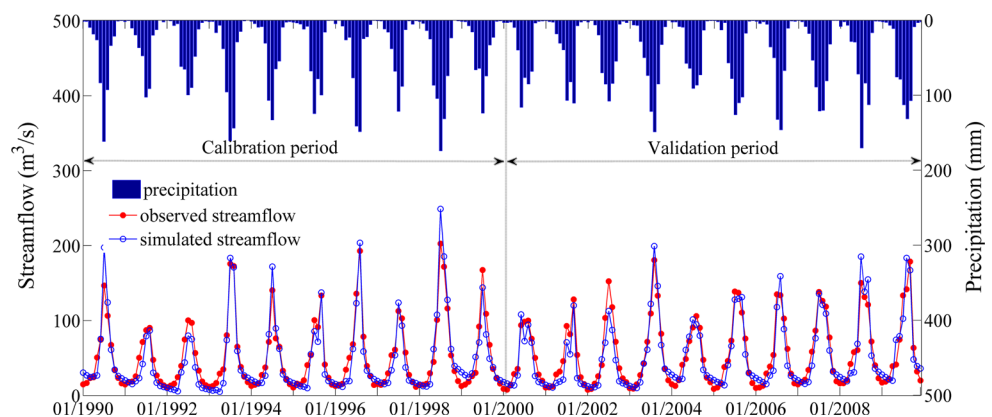
Fig. 4 Observed and simulated monthly streamflows during the calibration and validation periods at the Zhengyi Gorge station (outlet of the middle HRB) (Color figure online)
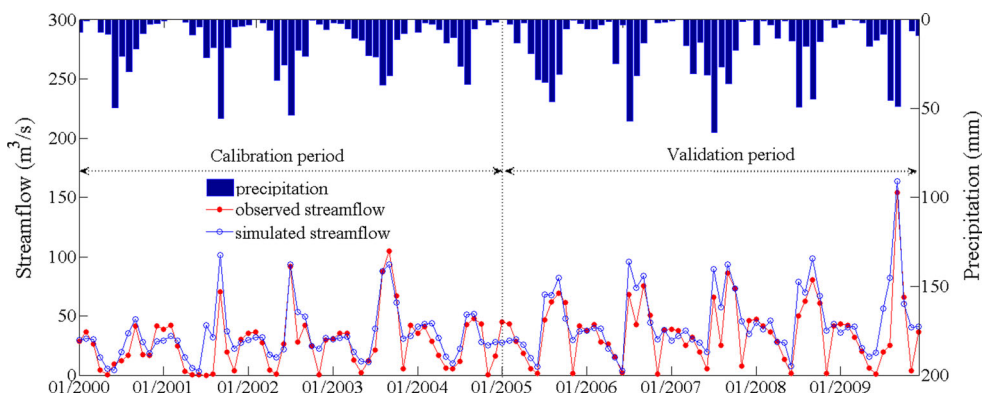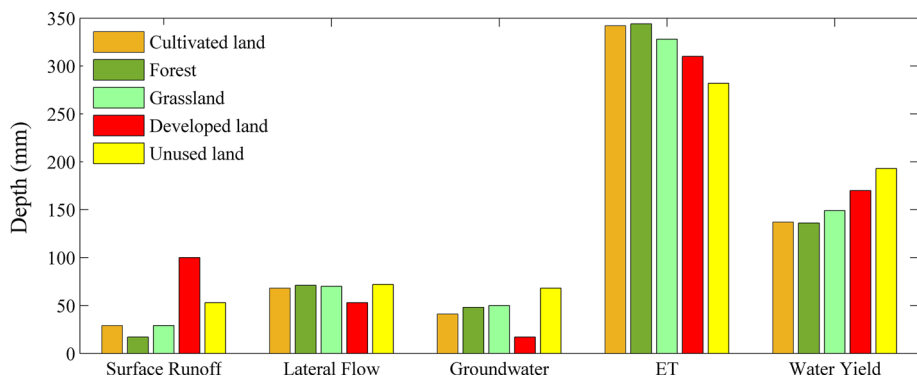

Fig. 5 Averaged simulated hydrological components for different land-use types from 1980 to 2009 (Color figure online)

lower runoff and water yield capacities than developed land, but higher than those of the forest.

Hydrological Responses to Land-Use Changes

Figure 6a depicts the changes in monthly mean streamflow relative to the baseline scenario at the outlet of the upper HRB, i.e., the Yingluo Gorge station, induced solely by various land-use change scenarios. The results reveal that the mean streamflow decreases from May to September

while barely changes from October to next April under all scenarios except for the SEP scenario. In the upper HRB, cultivated land and grassland which have a low water yield capacity appear to increase, while unused land with a high water yield capacity decreases under the HT, SP, and ED scenarios. These changes jointly result in decreased streamflow. Under the SEP scenario, a large area of unused land is converted to forest and grassland areas in the upper HRB, leading to a large increase in ET and a decrease in streamflow. The developed land area exhibits a large
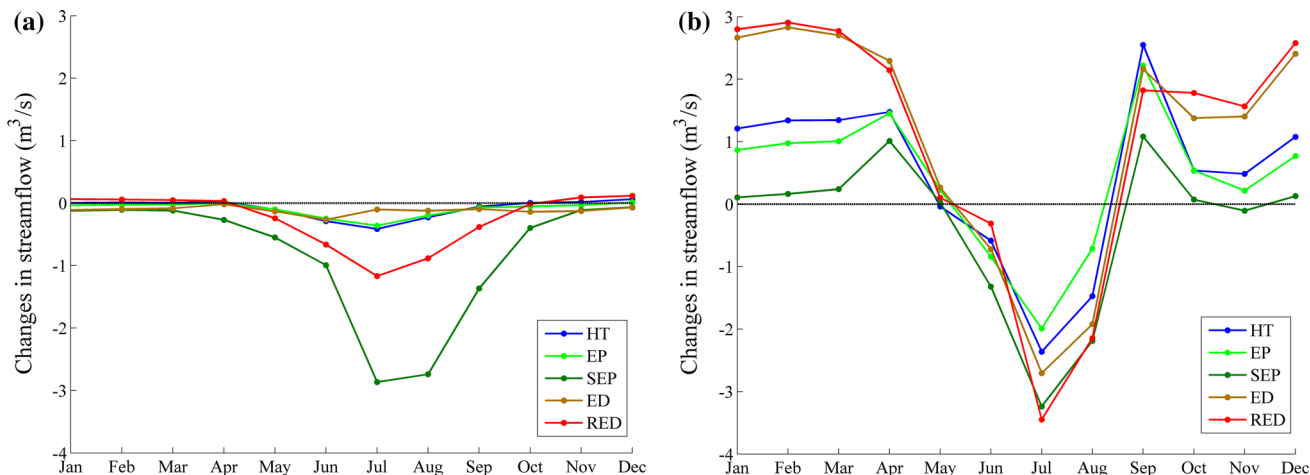
Fig. 6 Changes in mean monthly streamflows relative to the baseline scenario at the outlets of the upper HRB (**a**) and of the middle HRB (**b**) under constant climate condition (Color figure online)

Fig. 7 Mean monthly precipitations from 1980 to 2009 in the upper HRB (Color figure online)
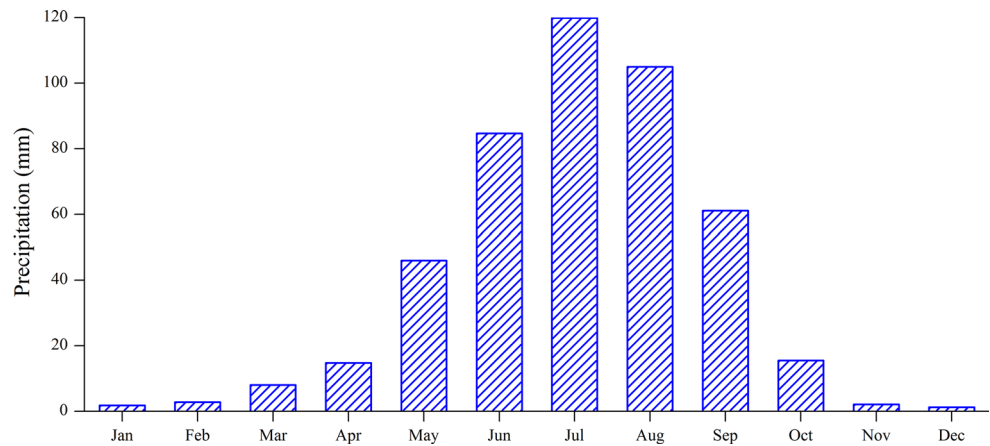
expansion under the RED scenario. However, the mean streamflow under this scenario shows a relatively obvious decrease trend from May to September. One explanation is that the increase of forest and grassland areas under this scenario will lead to rising ET and dropped streamflow. At the same time, the converted developed land is fragmentally distributed and leads to indistinct hydrological effects because the surface flow formed on impervious areas cannot be connected and later will infiltrate through the permeable zone. In addition, at some places even the expanded developed land links together, microclimate such as urban heat islands may increase the ET and decrease the streamflow (Fletcher et al. 2013).

As shown in Fig. 6a, the changes in mean streamflow relative to the baseline scenario are pronounced from June to September under all scenarios. The reason can be connected to the changes of ET and precipitation. The mean monthly ET is found to increase from June to September for all land-use scenarios. The largest increase occurs under the SEP scenario, followed by the RED, ED, EP and HT scenarios. Almost no changes can be discerned in other months under all scenarios. As a result, an obvious decrease of streamflow can be observed from June to September. As shown in Fig. 7, the precipitation is primarily concentrated in the same period, from June through September, in the upper HRB. Apart from the contribution of the changed ET, the pronounced change of streamflow in months with concentrated precipitation is possibly related to the high rainfall intensity but low soil moisture storage capacity following land-use changes (Li et al. 2013). In the months with scarce precipitation, small changes in ET, surface flow, and infiltration are detected, resulting in minor streamflow changes. The finding confirms the effects of land-use changes on streamflow vary with months (Fohrer et al. 2001).

Figure 6b presents the monthly streamflow changes at the outlet of the middle HRB, i.e., the Zhengyi Gorge station. The mean streamflow increases from December to

next April and decreases from Jun to August under all scenarios. The mean annual streamflow only decreases under the SEP scenario due to the increased forest area in the middle HRB and the reduced stream discharge from the upper HRB. The effects of land-use changes on streamflow are found to be strong in months with small precipitation, apparently different from that observed in the upper HRB. This finding can be explained by the intensive irrigation canal system which can enhance the impacts of land-use changes by increasing the return flows as a result of previous rotation irrigation.

The Pearson Type III peak-flow distributions for the Yingluo Gorge station under different scenarios are shown in Fig. 8a. Almost no change can be perceived in the peak-flow frequency distributions when comparing the HT, EP, ED, and RED scenarios with the baseline scenario. The results suggest that land-use changes under these scenarios almost have no impact on the frequency of extreme flood. However, the peak-flow frequency curve under the SEP scenario is present below the baseline scenario, implying a decreased frequency of the occurrence of extreme flood. For instance, a 100-year flood under the baseline scenario, namely a flood with a return period of 100 years (exceedance probability = 1 %), would occur less frequently if under the SEP scenario, which will be with a return period of about 154 years (exceedance probability = 0.65 %). Figure 8b depicts the minimum-flow frequency distributions. The frequency curves in different scenarios barely show any differences compared to the baseline scenario, meaning land-use change scenarios have very small impacts on the frequency of the occurrence of extreme drought.

Hydrological Responses to Land-Use and Climate Changes

Figure 9a presents the changes in mean monthly streamflow relative to the baseline scenario at the outlet of the
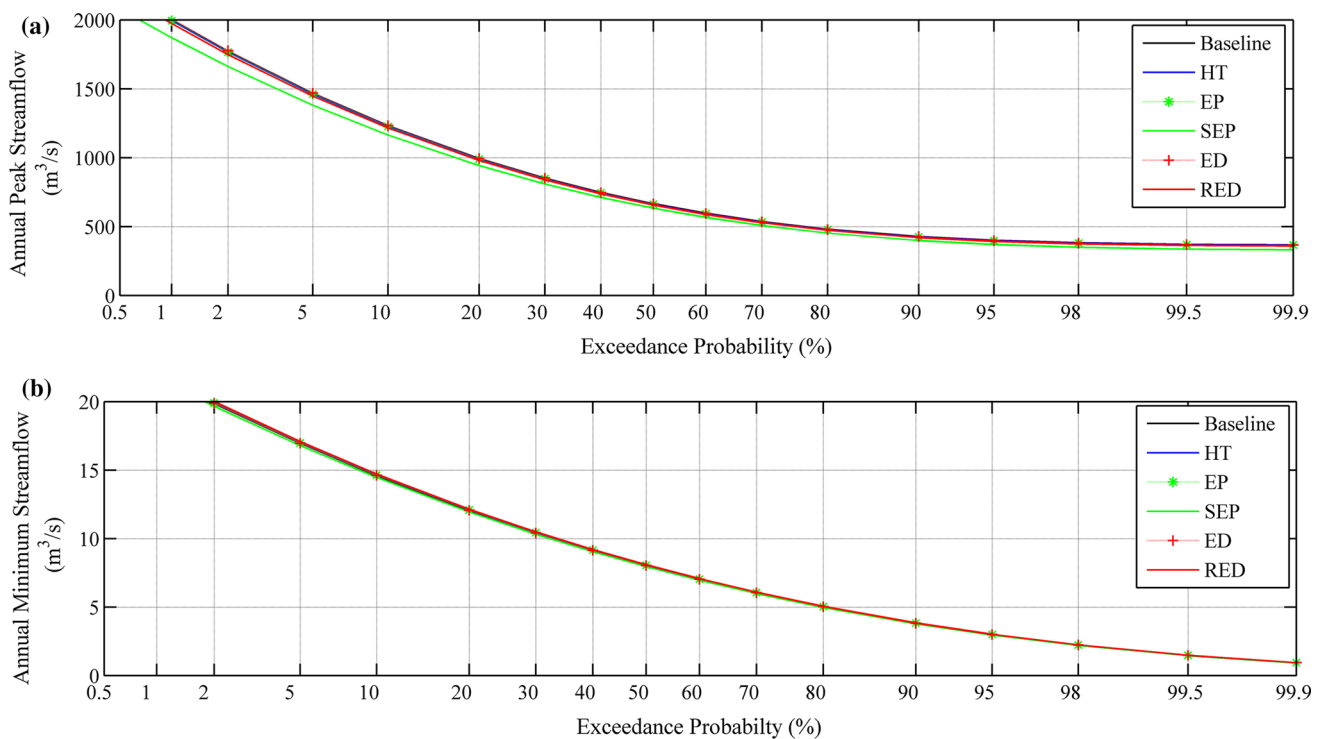
Fig. 8 Pearson Type III peak-flow (**a**) and minimum-flow (**b**) statistical distributions for the Yingluo Gorge station for different land-use scenarios under constant climate conditions (Color figure online)

upper HRB by jointly considering land-use changes and climate changes. The mean streamflow under all land-use scenarios. i.e., HT, EP, SEP, ED, and RED are projected to increase in June and September and decrease in other months for the A1B scenario of HadCM3 (Fig. 9a). The largest increase and decline occur in September and August, respectively. For the A1B scenarios of CGCM3 and CCSM3, the mean streamflow decreases almost in all months under all land-use scenarios. The drops can be up to 33.58 m^3/s in August for the CGCM3 A1B scenario and 29.39 m^3/s in July for the CCSM3 A1B scenario. Figure 9b shows the results under the B1 scenario of HadCM3, CGCM3, and CCSM3, where the mean streamflow are projected to decrease in most months. An increased trend can be found only in June and July for the CGCM3 B1 scenario and in August for the CCSM3 B1 scenario. As seen in Fig. 9, the changes look like to be grouped by climate scenarios; only within each group, impacts of land-use scenarios can be perceived. The finding supports that the impacts of land-use changes on streamflow become secondary when the changed climatic conditions are considered.

The comparison of mean monthly precipitation between the baseline and the climate scenario in the upper HRB are shown in Fig. 10a. Large changes can be observed from May to October. The largest increase (26.49 mm) and decrease (−12.64 mm) are projected by CGCM3 B1

scenario. Overall, the precipitation is projected to increase for the HadCM3 A1B, CGCM3 B1 and CCSM3 B1 scenarios, while for other scenarios, opposite trends can be found. By examining Figs. 10 and 9a, the large increase in precipitation can be reflected in the streamflow rises during the same months, whereas opposite trends are observed for the months with small precipitation increase. This is because the changes in streamflow are mainly induced by the changes in both precipitation and ET. Figure 11a shows the changes in mean monthly ET relative to the baseline in the same area. A large increasing trend of ET can be found from April to October, especially from June to September, under almost all the A1B and B1 scenarios of the GCMs. Generally, the ET is projected to increase. Such trend of increase, primarily driven by the increase in temperature projected by the GCMs, can offset the small increase of precipitation, bringing the streamflow down. Similar to the streamflow, the mean ET under the land-use scenarios (HT, ED, EP, and RED) is consistently changed with almost same magnitude for each climatic condition. The exception is the SEP scenario, in which the increase of ET in July and August is obviously larger than other land-use scenarios due to the existence of a larger area of forest.

The changes in mean monthly streamflow relative to the baseline scenario at the outlet of the middle HRB are present in Fig. 12a. The mean streamflow is projected to increase in most months for the HadCM3 A1B scenario.
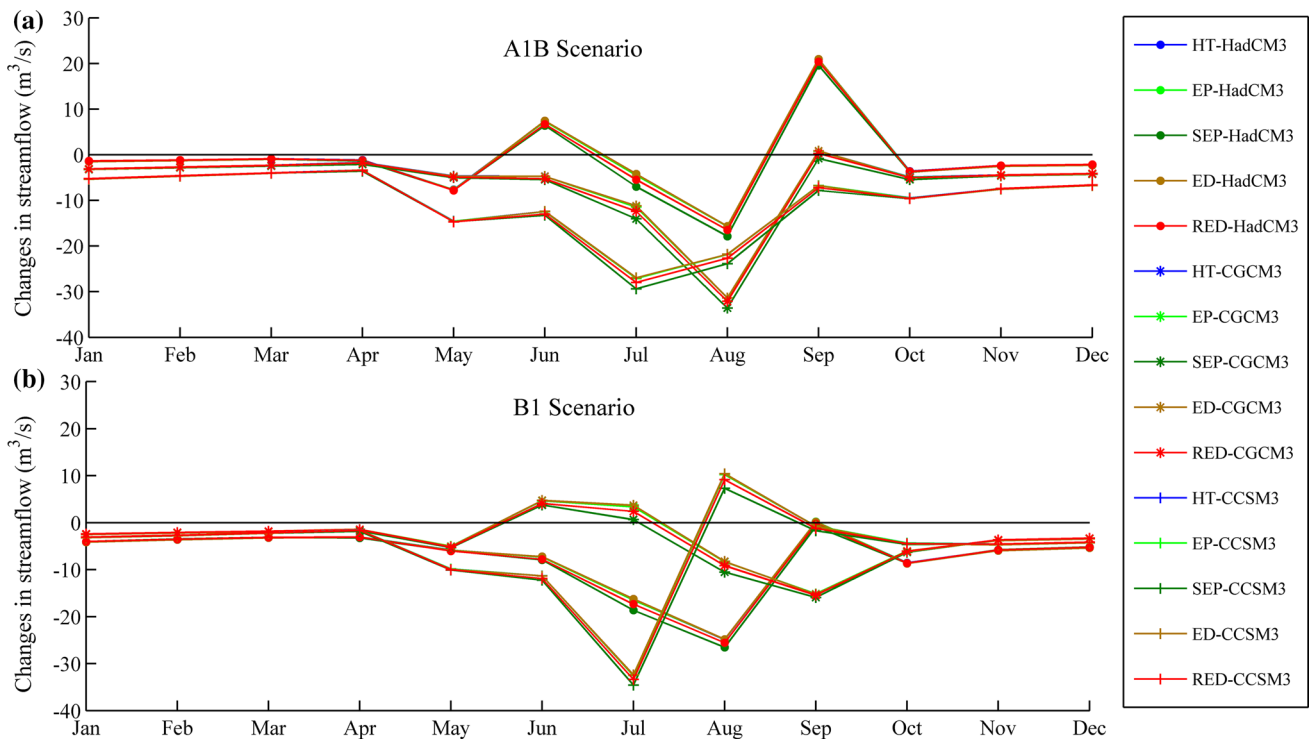
Fig. 9 Changes in mean monthly streamflows for combining land-use and climate change scenarios, A1B (**a**) and B1 (**b**), at the outlet of the upper HRB (Color figure online)

For the other A1B scenarios, however, streamflow declines during most months. Figure 12b depicts the results under the B1 scenarios of HadCM3, CGCM3, and CCSM3. Similarly, an increase trend projected by the HadCM3 and a decrease trend projected by the CGCM3 and CCSM3 can be found in most months. The largest increase is projected by HadCM3 with an increment of 16.89 m^3/s while the largest decrease is projected by the CCSM3 with a decrement of 27.39 m^3/s. Under the same climatic condition, the changes in mean streamflow are quite similar for all land-use scenarios. The results reconfirm that the streamflow is more sensitive to climate change than to land-use change. The comparison of mean monthly precipitation between the baseline and the climate scenario are shown in Fig. 10b. Large changes can be found from May to October as well. The largest increase and decrease under the A1B scenario are projected by the HadCM3 and CCSM3, respectively. The precipitation changes in the middle HRB is inconsistent with those in the upper HRB because of different geographical and climatic characteristics as well as uncertainties involved in the precipitation projections. As shown in Fig. 10b and 12, the precipitation changes can hardly be reflected in the streamflow changes. It can be explained by the increase of ET in the middle HRB and the changes of stream discharge from the upper HRB. Meanwhile, the irrigation canal system in the middle HRB can

also have large effects on streamflow generation at the outlet.

Figure 13a shows the Pearson Type III peak-flow distributions for the HT land-use scenario under different climatic conditions. The peak-flow frequency curves for the A1B and B1 scenarios of all GCMs are distributed below the baseline scenario when the exceedance probability is lower than 5 %. The results indicate a decreased frequency of extreme flood. The lowest frequency of extreme flood is projected by the CCSM3 under the A1B scenario. The minimum-flow frequency distributions for different climate scenarios are shown in Fig. 13b. All the frequency curves are appeared blow the baseline scenario, indicating a more frequent occurrence of extreme drought. For example, a 50-year drought with an assurance rate of 98 % (exceedance probability = 98 %) under baseline scenario would be return only in about 37 years (exceedance probability = 97.27 %) under the HadCM3 A1B scenario. The largest frequency of extreme drought is projected by the CGCM3 under the A1B scenario. The Pearson Type III peak-flow and minimum-flow distributions for other land-use scenarios, such as the EP, ED, and RED scenarios, almost overlap the HT scenario, in all the GCMs' climate scenarios. However, the frequency curve of the SEP scenario is present blow the HT scenario, suggesting a lower frequency of extreme flood and a higher frequency of extreme drought.
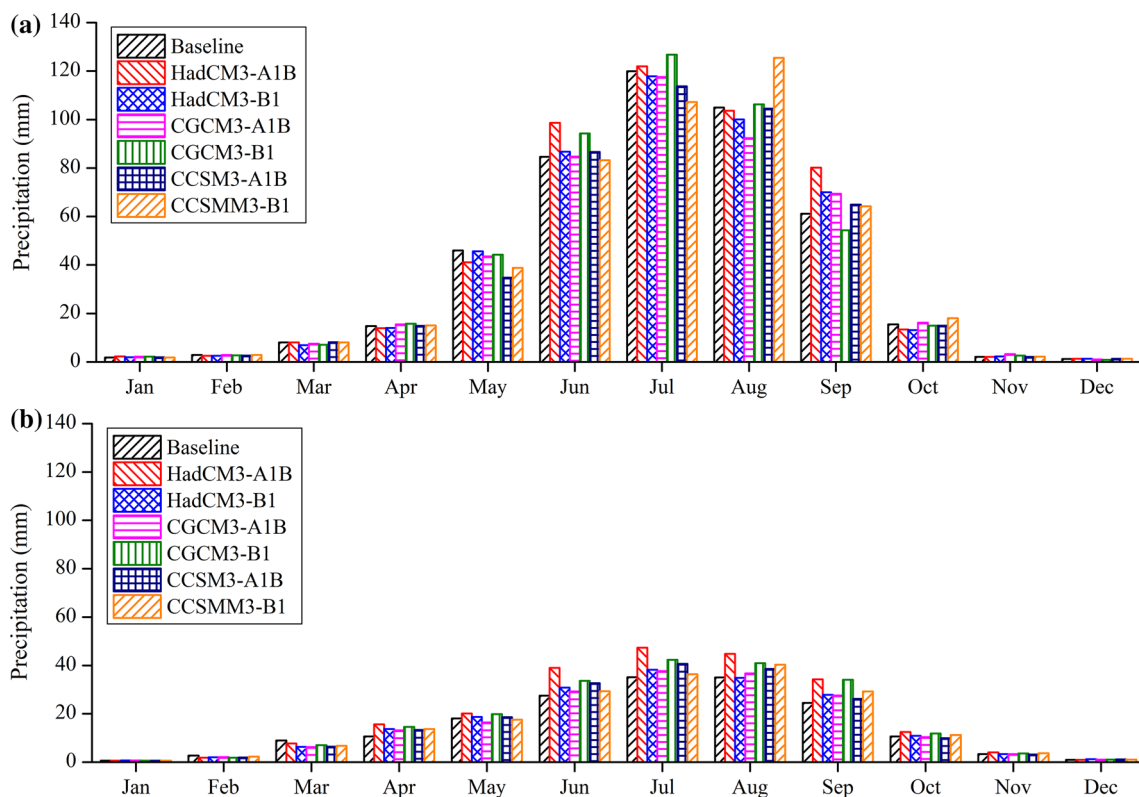
Fig. 10 Mean monthly precipitations for the baseline, and the A1B and B1 scenarios of three GCMs (HadCM3, CGCM3, and CCSM3) in the upper HRB (**a**), and the middle HRB (**b**) (Color figure online)
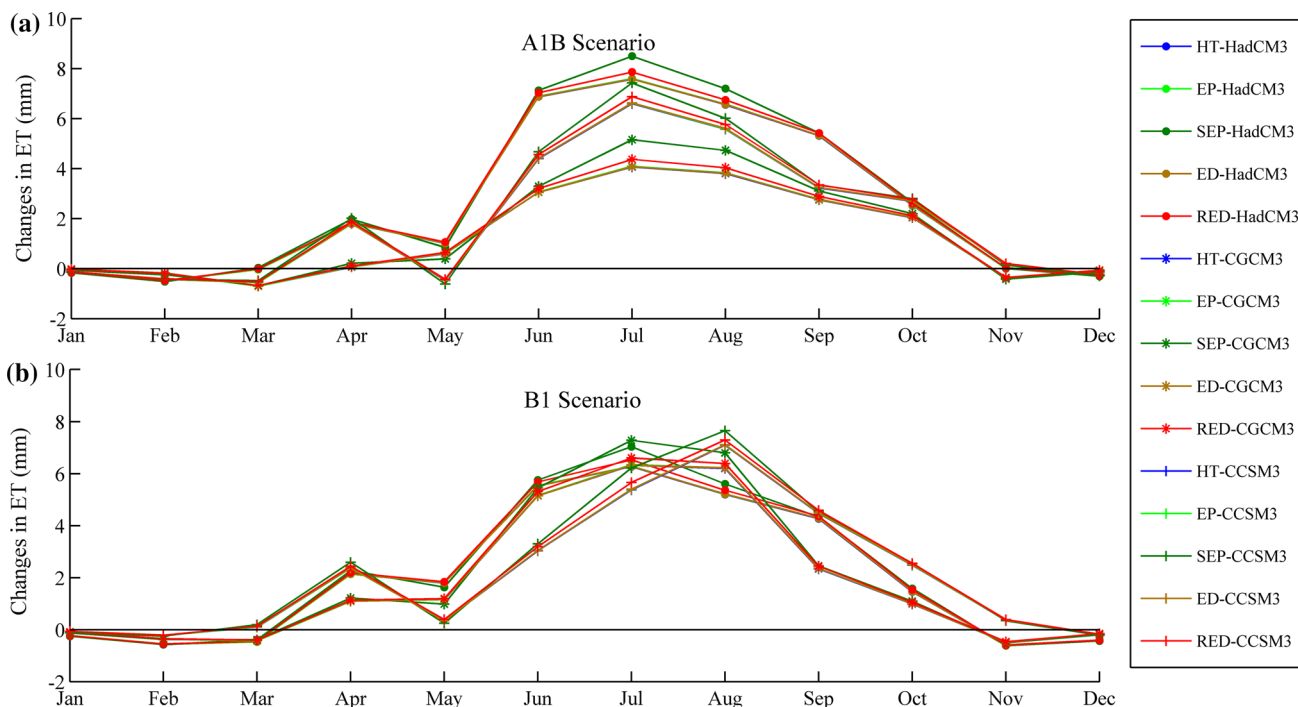

Fig. 11 Changes in mean monthly ETs for combining land-use change and climate change scenarios: A1B (**a**) and B1 (**b**), in the upper HRB (Color figure online)
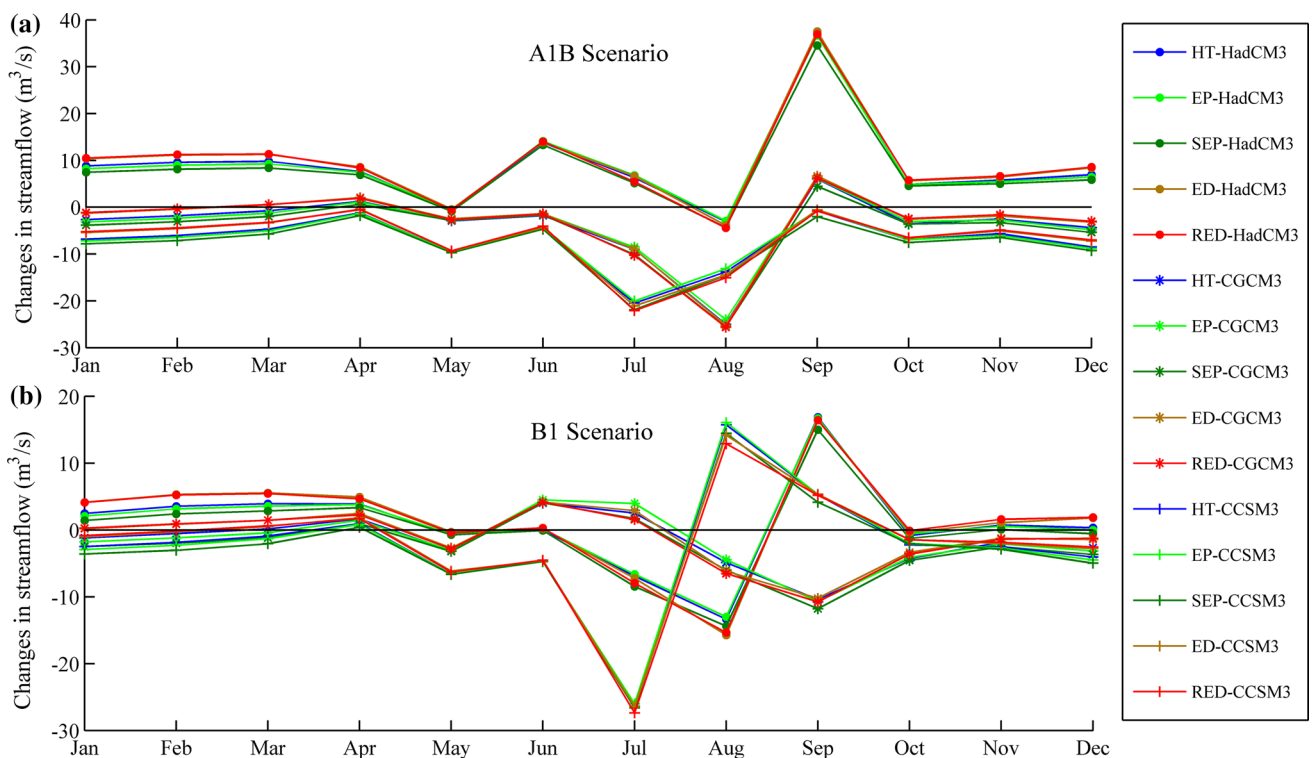
Fig. 12 Changes in mean monthly streamflow for combining land-use change and climate change scenarios, A1B (**a**) and B1 (**b**), at the outlet of the middle HRB (Color figure online)

Discussion

As present in "Hydrological Responses to Land-Use Changes" section, in the case of land-use changes under constant climatic condition, no substantial streamflow changes were simulated at the Yingluo Gorge station, ranging only from 2.35 to 0.56 %. It seems that land-use changes are not closely related to the changes in streamflow. The insensitivity of hydrological response can be explained by the following reasons. First, the absolute land-use changes are relatively small compared with the entire upper HRB under all land-use scenarios, so the affected areas are in fact relatively small. Second, the positive and negative impacts induced by the changes of land-use classes can offset each other, resulting in indistinct changes in streamflow at the outlet. We tested in a subbasin scale and recorded the changes at each outlets of subbasin. With a small area, the changes of mean monthly streamflow will fall into a larger range, from -14.03 to 5.83 %. That means more pronounced changes are perceived on a subbasin level, in alignment with what those presented in other studies (Hurkmans et al. 2009; Wagner et al. 2013).

In "Hydrological Responses to Land-Use and Climate Changes" section, where we have examined the hydrological responses to land-use changes in combination with changed climatic conditions, one of our findings is that the streamflow and extremes respond more sensitively to climate change than to land-use change. The impacts of land-use changes on hydrological variations become secondary when changed climatic conditions have been taken into consideration. In our case, the future climatic condition of two emission (A1B and B1) scenarios was established by downscaling precipitation and temperature projected by three GCMs (HadCM3, CGCM3, and CCSM3). It is noticed that the projected precipitation varies with GCMs and emission scenarios. The uncertainty in projected precipitation is large. Figure 10 shows the changes in mean precipitation in the middle HRB, which appear smoother than in the upper HRB. The difference possibly lies on their different geographical and climatic characteristics. It implies large uncertainties of projected precipitation exist in GCMs when downscaling is performed in mountainous area. The stronger spatial heterogeneity in the upper HRB may lead to a larger uncertainty in projected precipitation (Chen 2002). Unlike the large variations in projected precipitation, however, a general increase trend of temperature is projected for all the climate change scenarios in the entire study area. Those uncertainties may also be responsible for the inconsistent changes in streamflow and hydrological extremes for different GCMs and emission scenarios. Although we cannot conclude a simple
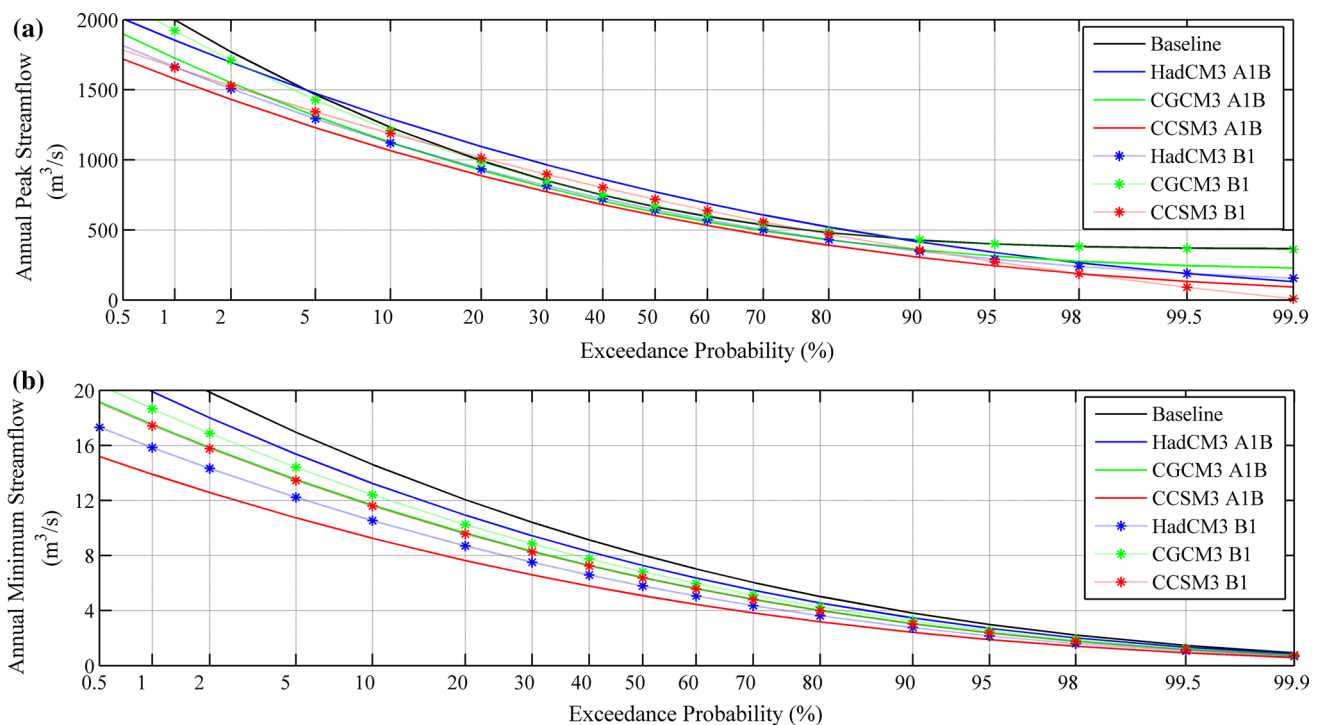
Fig. 13 Pearson Type III peak-flow (**a**) and minimum-flow (**b**) statistical distributions for the HT scenario under the A1B (**a**) and B1 (**b**) climate scenarios projected by HadCM3, CGCM3, and CCSM3 (Color figure online)

conclusion regarding the impact of climate change on streamflow and hydrological extremes due to difficulty in evaluating uncertainties in those GCMs, some interesting points still can be reached. It necessitates the need of multiple scenarios and GCMs in assessing the impacts of climate change on hydrological variations. For example, the HadCM3 A1B scenario will conclude an obvious increase of streamflow in response to climate changes as shown in Fig. 12, while other climate change scenarios may conclude opposite results. In addition, processing method and assumptions also bring uncertainty to the results. Uncertainties sourced from different downscaling methods, hydrological model, and baseline periods need to be evaluated further. In this study, the calibration of hydrological model was conducted only for a special time period and land-use configuration. Thus, one implicit assumption in this study is that the calibrated parameters are still valid and applicable for future land-use and climatic conditions. However, this assumption may not hold good. For example, the large increase in grassland and forest areas may make the calibrated parameters related to ET, such as the soil evaporation compensation factor (ESCO), to be no longer applicable. Similarly, the parameters may potentially change when the climatic condition has been changed (Merz et al. 2011).

In the upper HRB, few human activities have occurred in the mountainous area so far. Climate change plays the

most important role in changing the streamflow at the outlet (Zhang et al. 2015). In our case, except for the HadCM3 A1B scenario, all other climate scenarios project a decreasing trend of stream discharge from the upper HRB. This result may bring much attention to the local water source managers. As we mentioned in "Study Area" section, the middle HRB, supports millions of people, is the major water consumer, accounting for approximately 90 % of the total water use from the Heihe River. However, very few streamflow can be generated in this region due to low precipitation and high evapotranspiration. As a result, the stream discharge from the upper HRB becomes the most important water resource for the middle HRB. If the projected result of our study actually occurs, then water stress in the middle HRB, which has been enhanced by intensive human activities, will become more severe. As a typical inland river basin in the arid region, the HRB owns common geographic and climatic characteristics of inland basin in arid region. The water stresses are also commonly found in other arid region. Thus, the impact assessments of land-use and climate changes on hydrology may be of common interest to similar basins across the world.

The five land-use scenarios that represent a range of tradeoffs between ecological protection and economic development were carefully established based on the local governmental planning and relevant research results. The results of this study therefore will be meaningful for land

and water resource management in HRB. Nevertheless, there are some spaces for improvement regarding the scenario settings. The results would be more instructive and valuable for decision making, if the land-use demands could be estimated according to survey data of each administrative area instead of coarse overall estimates of the entire region. The spatial restrictions and modeling could be improved if more incentives are included. Although two emission scenarios from three GCMs were employed to estimate possible climatic conditions in the future, it is still challenging to advice which results are most likely to happen so that the stakeholders can prepare to take adaptive measures to mitigate possible risks.

Conclusions

The hydrological responses to land-use change scenarios under constant and changed climatic conditions were examined by combining the Dyna-CLUE and SWAT models in the upper and middle HRB, which is a typical inland river basin in the arid northwest China sharing many water problems like in other arid regions worldwide. The following conclusions can be drawn from this study.

(1) Both the LUCC model, Dyna-CLUE, and the hydrological model, SWAT, are validated to be applicable in the study area in assessing the hydrological responses to land-use and climate changes. Modeled with Dyna-CLUE, distinct land-use changes will be present in 2039 under the two extreme scenarios, i.e., strict ecological protection (SEP) and rapid economic development (RED) scenarios. Other scenarios, such as historic trend (HT), ecological protection (EP), and economic development (ED) scenarios, however, only show slight changes.

(2) In cases where hydrological responses are solely induced by land-use changes while keeping climatic condition constant, the mean streamflow at the outlet of the upper HRB decreases in most months under each and every land-use scenarios. The streamflow changes at the outlets of both the upper and the middle HRB are not pronounced. However, more pronounced streamflow changes can be perceived on a subbasin level. Moreover, the effects of land-use changes on streamflow are observed to vary over differrent months. In this constant climate case, the frequency of extreme flood is projected to decrease under the SEP scenario, while under other land-use scenarios, almost no change can be found.

(3) In a more realistic case, hydrological responses are induced by the combined effects of land-use and climate changes, in which climate changes play a dominant role in impacting streamflow and hydrological extremes, while the land-use changes take the second place. Although some agreements can be reached, pronounced difference of hydrological responses can be observed for different climate scenarios of different GCMs, as a result of uncertainty in projected precipitation and temperature. The frequencies of occurrence of extreme flood and drought are projected to decrease and increase, respectively, for all the climate scenarios.

Understanding the impacts of land-use and climate changes is crucial for sustainable water resource management. The findings of this study will provide useful information for planners and policy makers in planning and managing the land and water resources in HRB and have valuable implications for similar inland river basins in arid regions which experience common water problems.

References

Ashraf Vaghefi S, Mousavi S, Abbaspour K, Srinivasan R, Yang H (2014) Analyses of the impact of climate change on water resources components, drought and wheat yield in semiarid regions: Karkheh River Basin in Iran. Hydrol Process 28:2018–2032. doi:10.1002/hyp.9747

Baker TJ, Miller SN (2013) Using the Soil and Water Assessment Tool (SWAT) to assess land use impact on water resources in an East African watershed. J Hydrol 486:100–111. doi:10.1016/j.jhydrol.2013.01.041

Chen W (2002) The hydrological characteristics of Heihe River Basin (in Chinese). Hydrology 22:57–60

Chu HJ, Lin YP, Huang CW, Hsu CY, Chen HY (2010) Modelling the hydrologic effects of dynamic land-use change using a distributed hydrologic model and a spatial land-use allocation model. Hydrol Process 24:2538–2554. doi:10.1002/hyp.7667

Dai S, Zhang B (2013) Land use change scenarios simulation in the middle reaches of the Heihe River Basin based on CLUE-S model—a case of Ganzhou district of Zhangye city (in chinese). J Nat Resour 28:336–348

Diaz-Nieto J, Wilby RL (2005) A comparison of statistical downscaling and climate change factor methods: impacts on low flows in the River Thames, United Kingdom. Clim Change 69:245–268. doi:10.1007/s10584-005-1157-6

Dixon B, Earls J (2012) Effects of urbanization on streamflow using SWAT with real and simulated meteorological data. Appl Geogr 35:174–190. doi:10.1016/j.apgeog.2012.06.010

Du J et al (2013) Hydrological simulation by SWAT model with fixed and varied parameterization approaches under land use change. Water Resour Manag 27:2823–2838. doi:10.1007/s11269-013-0317-0

Elfert S, Bormann H (2010) Simulated impact of past and possible future land use changes on the hydrological response of the Northern German lowland 'Hunte' catchment. J Hydrol 383:245–255. doi:10.1016/j.jhydrol.2009.12.040

Fang C, Bao C (2004) The coupling model of water-ecology-economy coordinated development and its application in Heihe River Basin (in Chinese). Acta Geogr Sinica 59:781–790

Ficklin DL, Stewart IT, Maurer EP (2013) Effects of projected climate change on the hydrology in the Mono Lake Basin, California. Clim Change 116:111–131. doi:10.1007/s10584-012-0566-6

Fletcher T, Andrieu H, Hamel P (2013) Understanding, management and modelling of urban hydrology and its consequences for receiving waters: a state of the art. Adv Water Resour 51:261–279. doi:10.1016/j.advwatres.2012.09.001

Fohrer N, Haverkamp S, Eckhardt K, Frede H-G (2001) Hydrologic response to land use changes on the catchment scale. Phys Chem Earth Part B 26:577–582. doi:10.1016/S1464-1909(01)00052-1

Fotakis D, Sidiropoulos E, Loukas A (2014) Integration of a hydrological model within a geographical information system: application to a forest watershed. Water 6:500–516. doi:10.3390/w6030500

Gobin A, Campling P, Feyen J (2002) Logistic modelling to derive agricultural land use determinants: a case study from southeastern Nigeria. Agric Ecosyst Environ 89:213–228. doi:10.1016/S0167-8809(01)00163-3

Guo B, Zhang J, Song L, Gong H (2012) Hydrologic Scenario Simulation and Related Techniques Forecasting Land Use/Land Cover Changes. In: Remote Sensing, Environment and Transportation Engineering (RSETE), 2012 2nd International Conference on 2012. IEEE, pp 1-4. doi:10.1109/RSETE.2012.6260589

Hay LE, Wilby RL, Leavesley GH (2000) A comparison of delta change and downscaled GCM scenarios for three mountainous basins in the United States. J Am Water Resour Assoc 36:387–397. doi:10.1111/j.1752-1688.2000.tb04276.x

Hurkmans R, Terink W, Uijlenhoet R, Moors E, Troch P, Verburg P (2009) Effects of land use changes on streamflow generation in the Rhine basin. Water Resour Res. doi:10.1029/2008WR007574

Im S, Kim H, Kim C, Jang C (2009) Assessing the impacts of land use changes on watershed hydrology using MIKE SHE. Environ Geol 57:231–239. doi:10.1007/s00254-008-1303-3

Khoi DN, Suetsugi T (2014) The responses of hydrological processes and sediment yield to land-use and climate change in the Be River Catchment, Vietnam. Hydrol Process 28:640–652

Kim J, Choi J, Choi C, Park S (2013) Impacts of changes in climate and land use/land cover under IPCC RCP scenarios on streamflow in the Hoeya River Basin, Korea. Sci Total Environ 452:181–195. doi:10.1016/j.scitotenv.2013.02.005

Lai Z, Li S, Li C, Nan Z, Yu W (2013) Improvement and applications of SWAT Model in the upper-middle Heihe River Basin (in Chinese). J Nat Resour 28:1404–1413

Lehner B, Döll P, Alcamo J, Henrichs T, Kaspar F (2006) Estimating the impact of global change on flood and drought risks in Europe: a continental, integrated analysis. Clim Change 75:273–299. doi:10.1007/s10584-006-6338-4

Li X, Lu L, Cheng G, Xiao H (2001) Quantifying landscape structure of the Heihe River Basin, north-west China using FRAGSTATS. J Arid Environ 48:521–535. doi:10.1006/jare.2000.0715

Li Z, Xu Z, Shao Q, Yang J (2009) Parameter estimation and uncertainty analysis of SWAT model in upper reaches of the Heihe river basin. Hydrol Process 23:2744–2753. doi:10.1002/hyp.7371

Li L, Jiang D, Hou X, Li J (2013) Simulated runoff responses to land use in the middle and upstream reaches of Taoerhe River basin, Northeast China, in wet, average and dry years. Hydrol Process 27:3484–3494. doi:10.1002/hyp.9481

Liston GE, Elder K (2006) A meteorological distribution system for high-resolution terrestrial modeling (MicroMet). J Hydrometeorol 7:217–234. doi:10.1175/JHM486.1

Mango L, Melesse A, McClain M, Gann D, Setegn S (2011) Land use and climate change impacts on the hydrology of the upper Mara River Basin, Kenya: results of a modeling study to support better resource management. Hydrol Earth Syst Sci. doi:10.5194/hess-15-2245-2011

Merz R, Parajka J, Blöschl G (2011) Time stability of catchment model parameters: implications for climate impact analyses. Water Resour Res. doi:10.1029/2010WR009505

Moriasi D, Arnold J, Van Liew M, Bingner R, Harmel R, Veith T (2007) Model evaluation guidelines for systematic quantification of accuracy in watershed simulations. Trans ASABE 50:885–900

Nash J, Sutcliffe JV (1970) River flow forecasting through conceptual models part I—a discussion of principles. J Hydrol 10:282–290

Neitsch SL, Arnold JG, Kiniry JR, Williams JR (2011) Soil and Water Assessment Tool theoretical documentation: Version 2009. Texas Water Resources Institute. http://hdl.handle.net/1969.1/128050

Nejadhashemi A, Wardynski B, Munoz J (2011) Evaluating the impacts of land use changes on hydrologic responses in the agricultural regions of Michigan and Wisconsin. Hydrol Earth Syst Sci Dis 8:3421–3468

Nian Y, Li X, Zhou J, Hu X (2014) Impact of land use change on water resource allocation in the middle reaches of the Heihe River Basin in northwestern China. J Arid Land 6:273–286. doi:10.1007/s40333-013-0209-4

Nie W, Yuan Y, Kepner W, Nash MS, Jackson M, Erickson C (2011) Assessing impacts of Landuse and Landcover changes on hydrology for the upper San Pedro watershed. J Hydrol 407:105–114. doi:10.1016/j.jhydrol.2011.07.012

Park J, Park M, Joh H, Shin H, Kwon H, Srinivasan R, Kim S (2011) Assessment of MIROC 3. 2 HiRes climate and CLUE-s land use change impacts on watershed hydrology using SWAT. Transactions of the ASABE 54:1713–1724

Perazzoli M, Pinheiro A, Kaufmann V (2013) Assessing the impact of climate change scenarios on water resources in southern Brazil. Hydrol Sci J 58:77–87. doi:10.1080/02626667.2012.742195

Serneels S, Lambin EF (2001) Proximate causes of land-use change in Narok District, Kenya: a spatial statistical model. Agric Ecosyst Environ 85:65–81. doi:10.1016/S0167-8809(01)00188-8

Shanghai Urban Planning & Design Institute, Zhangye Urban Construction Commission (2004) Urban Planning Outline of Zhangye City for 2004 to 2020 (in Chinese)

Shi P et al (2013) Effects of land-use and climate change on hydrological processes in the Upstream of Huai River, China. Water Resour Manag 27:1263–1278. doi:10.1007/s11269-012-0237-4

Sriwongsitanon N, Taesombat W (2011) Effects of land cover on runoff coefficient. J Hydrol 410:226–238. doi:10.1016/j.jhydrol.2011.09.021

Tanzeeba S, Gan TY (2012) Potential impact of climate change on the water availability of South Saskatchewan River Basin. Clim Change 112:355–386. doi:10.1007/s10584-011-0221-7

The Ministry of Water Resources of the People's Public of China (2000) Recent management planning of Heihe River Basin (in Chinese). China Water Power Press, Beijing

The People's Government of Zhangye (2012) Development planning outline of Zhangye City towards a well-being and tourist city for 2012 to 2020 (in Chinese)

Tong ST, Sun Y, Ranatunga T, He J, Yang YJ (2012) Predicting plausible impacts of sets of climate and land use change

scenarios on water resources. Appl Geogr 32:477–489. doi:10.1016/j.apgeog.2011.06.014

Verburg PH, Overmars KP (2009) Combining top-down and bottom-up dynamics in land use modeling: exploring the future of abandoned farmlands in Europe with the Dyna-CLUE model. Landsc Ecol 24:1167–1181. doi:10.1007/s10980-009-9355-7

Verburg PH, Soepboer W, Veldkamp A, Limpiada R, Espaldon V, Mastura SSA (2002) Modeling the spatial dynamics of regional land use: the CLUE-S model. Environ Manag 30:391–405. doi:10.1007/s00267-002-2630-x

Verburg PH, de Nijs T, Ritsema van Eck J, Visser H, de Jong K (2004) A method to analyse neighbourhood characteristics of land use patterns. Comput Environ Urban Syst 28:667–690. doi:10.1016/j.compenvurbsys.2003.07.001

Verburg PH, Overmars KP, Huigen MGA, de Groot WT, Veldkamp A (2006) Analysis of the effects of land use change on protected areas in the Philippines. Appl Geogr 26:153–173. doi:10.1016/j.apgeog.2005.11.005

Wagner P, Kumar S, Schneider K (2013) An assessment of land use change impacts on the water resources of the Mula and Mutha Rivers catchment upstream of Pune, India. Hydrol Earth Syst Sci 17:2233–2246. doi:10.5194/hess-17-2233-2013

Wan R, Yang G (2005) Discussion on some issues of hydrological effects of watershed land use and land cover change (in Chinese). Process Geogr 24:25–33

Wang L, Zhang X (2010) Effect of the recent climate change on water resource in Heihe river basin (in Chinese). J Arid Land Resour Environ 24:60–65

Wang G, Yang L, Chen L, Jumpei K (2005) Impacts of land use changes on groundwater resources in the Heihe River Basin. J Geogr Sci 15:405–414. doi:10.1007/BF02892147

Wang G, Liu J, Kubota J, Chen L (2007) Effects of land-use changes on hydrological processes in the middle basin of the Heihe River, northwest China. Hydrol Process 21:1370–1382. doi:10.1002/hyp.6308

Wang Y, Yan C, Wang J (2011) Landuse/Landcover data of the Heihe river basin in 2000. Heihe Plan Science Data Center. doi:10.3972/heihe.020.2013.db

Wang G, Yang H, Wang L, Xu Z, Xue B (2014) Using the SWAT model to assess impacts of land use changes on runoff generation in headwaters. Hydrol Process 28:1032–1042. doi:10.1002/hyp.9645

Wen H, Li Q, Li P, Cai T (2013) Analysis of impact of land use change on runoff characteristics (in Chinese). Water Resour Power 31:12–14

Wijesekara G, Gupta A, Valeo C, Hasbani J-G, Qiao Y, Delaney P, Marceau D (2012) Assessing the impact of future land-use changes on hydrological processes in the Elbow River watershed in southern Alberta, Canada. J Hydrol 412:220–232. doi:10.1016/j.jhydrol.2011.04.018

Wilby RL, Hay LE, Leavesley GH (1999) A comparison of downscaled and raw GCM output: implications for climate change scenarios in the San Juan River basin, Colorado. J Hydrol 225:67–91. doi:10.1016/S0022-1694(99)00136-5

Xia J, Tan G (2002) Hydrological science towards global change:progress and challenge (in Chinese). Resour Sci 24:1–7

Xu L, Li Z, Song H, Yin H (2013a) Land-use planning for Urban Sprawl based on the CLUE-S model: a case study of Guangzhou, China. Entropy 15:3490–3506. doi:10.3390/e15093490

Xu Y-P, Zhang X, Ran Q, Tian Y (2013b) Impact of climate change on hydrology of upper reaches of Qiantang River Basin, East China. J Hydrol 483:51–60. doi:10.1016/j.jhydrol.2013.01.004

Zang C, Liu J (2013) Trend analysis for the flows of green and blue water in the Heihe River basin, northwestern China. J Hydrol 502:27–36. doi:10.1016/j.jhydrol.2013.08.022

Zhang K, Wang R, Han H, Wang X, Si J (2007) Hydrological and water resources effects under climate change in Heihe River Basin (in Chinese). Resour Sci 01:77–83

Zhang A, Zheng C, Wang S, Yao Y (2015) Analysis of streamflow variations in the Heihe River Basin, northwest China: trends, abrupt changes, driving factors and ecological influences. J Hydrol 3:106–124. doi:10.1016/j.ejrh.2014.10.005

Zhou F, Xu Y, Chen Y, Xu C-Y, Gao Y, Du J (2013) Hydrological response to urbanization at different spatio-temporal scales simulated by coupling of CLUE-S and the SWAT model in the Yangtze River Delta region. J Hydrol 485:113–125. doi:10.1016/j.jhydrol.2012.12.040